Proceedings of the ASPF 2003 (The 8th Asian Symposium on Precision Forging), October 15 - 18, 2003

MICRO HOLE FABRICATION BY MECHANICAL PUNCHING PROCESS

B. Y. Joo[1], S. H. Rhim[1], S. I. Oh[2]

Abstract

The objective of our study is to investigate the micro fabricability by conventional metal forming processes. In the present investigation, micro hole punching was studied. We tried to control punching process at the micro level and scaled down the standard blanking condition for 25㎛ hole fabrication. To accommodate this, tungsten carbide tooling sets and micro punching press were carefully designed and assembled meeting accuracy requirements for 25 ㎛ hole punching. With our developments, 100, 50, and 25㎛ holes were successfully made on metal foils such as brass and stainless steel of 100, 50, and 25㎛ in thickness, respectively, and hole sizes and shapes were measured and analyzed to investigate fabrication accuracy. Shear behavior during micro punching was also discussed. Our study showed that the conventional punching process could produce high quality holes down to 25㎛.

Keywords : micro hole, punching, alignment

1. Introduction

Metal forming technology has the potential applicability in micro scale applications due to its process simplicity and high production capability. For this reason, micro fabrications by various press-working processes such as micro forging [1-2], micro coining [3-4], and micro sheet metal forming [5-6] have been attempted.

In this paper, micro punching was studied because mechanical punching processes for several hundred micron holes are already fabricated in the manufacturing industry, and there has been increasing demands for subhundred micron holes. However, mechanical punching of holes of several tens of microns is still in the research stages [7-8] because of the difficulty in fabricating tools and meeting the accuracy requirements of the press system.

We accommodated the fabrication of micro holes having the thickness-to-diameter ratio of one on metal foils by mechanical punching process. Basically, we tried to control both the feature size and blanking process condition [9] such as the ratio of punch-to-die clearance to workpiece thickness, c/t=5%, and scaled it down to 25㎛ hole punching process. We chose 25㎛ as the smallest feature size, because c/t=5% requires the punch-to-die clearance of only 1㎛ for 25㎛ hole fabrication. We have developed the micro punching system [10]. To ensure process accuracy at the micron level, we avoided the conventional press system, but rather a flexible system was designed and assembled in a way that a micro punch could have highly accurate vertical motion, and a die plate was mounted on the movable x-y stepper for adjusting the tool alignment purpose. The tool alignment was to be verified with the help of a vision system.

[1] Graduate school, Seoul national univ., Korea
[2] School of mechanical and aerospace eng., Seoul national univ., Korea

However, previous system was designed considering process accuracy for 100㎛ hole punching, and fabrication of 25㎛ hole still remained to be a challenge.

To accommodate 25㎛ hole punching, tungsten carbide tooling sets were designed and fabricated by micro machining process, and a press system was designed to meet the accuracy requirements for 25㎛ hole punching. To ensure the straight vertical motion of a punch, a punch-moving part was carefully designed, considering the kinematic design principle and minimizing punch run-out considering Abbe error [15] at the punch tip. Also, a tool alignment teacher using two-way image acquisition was newly developed for tool alignment purpose. With our developments, 100, 50, 25㎛ holes were successfully made on metal foils such as brass and stainless steel of 100, 50, 25㎛ in thickness, respectively, and their sizes and shapes were measured and analyzed to investigate fabrication accuracy. Fabrication results showed that the mechanical punching process could make high quality holes even in micro scale application at high reproducibility.

2. Machine design ensuring process accuracy

2.1 Design and fabrication of micro tools

For high rigidity and edge stability of micro punching tools, ultra fine graded tungsten carbide was chosen as the tool material having the compressive strength, bending strength, and elastic modulus of 6.5, 3.8 and 560GPa, respectively. To design 25㎛ punch tip, we calculated the punch load as given by (1) for 25㎛ hole punching on metal foil of 25㎛ in thickness.

$$F_p \le \pi DHS_f S_u \tag{1}$$

where D, H, S_u, S_f are the hole size, hole depth, tensile strength of the workpiece, and the shear factor with the range of 0.7~0.8, respectively [12]. To obtain the maximum punch load, the tensile strength of stainless steel foil was used and S_f=1 so that $F_{p,max}$=1.7N. Next, to decide the tool tip length, buckling and bending failure at the tool tip under maximum punch load were considered so that 25㎛ punch tip of 50㎛ in length was designed. With similar design guides, for the case of 50 and 100㎛ hole punching, maximum punch loads were also calculated as about 6.8 and 27N, respectively, and punch tip of 50㎛ in diameter and 100㎛ in length, and 100㎛ in diameter and 200㎛ in length were designed, respectively. To accommodate good surface roughness and edge sharpness of punch tip, micro punches were machined by ultra precision micro grinder, and dimensional tolerances of tool tip diameter were to be within 1㎛. Fig.1-(a), (c), and (e) show the micro ground punch tips. Satisfactorily enough, their surface roughness and edges sharpness were qualitatively acceptable in micro scale application. However, the 25㎛ punch tip did not seem to have a straight shank, but rather a relatively tapered on was observed, and such error was thought to be due to the machining limit of a micro grinder. Some squareness errors between the tip shank and its bottom were also observed. However, we did not care about this kind of error, because we expected that it would work as the shear angle of a punch [13]. A micro punch was designed to have three steps. The first step was punch tip. The second step was to have a diameter of 300㎛ and length of 1.5mm, which corresponded to the thickness of stripper plate. To be mounted on a punch gripper, the third step was to have a diameter of 800㎛ and length of 15mm. Also, each intra steps of a punch was tapered at about 17° to ensure its structural safety as shown in Fig.1-(g).

A die holder was made of AISI D2 block of 80×40×10mm in size, and mounted on movable x-y stepper of punching machine. At the center of die block, a longitudinal channel of 7mm

wide and 20mm long was machined. For ensuring flatness and parallelism, its upper and lower sides were precisely ground. To meet the standard blanking condition, c/t=5%, a die hole of 27, 55, and 110μm in diameter were necessary. As a die, tungsten carbide plate of dimensions 15×15×1mm was used, and the upper side of die plate was carefully polished with submicron diamond abrasive. Die hole was designed to have the ratio of hole depth to diameter of around one. For fabricating this, first, a counter bore of about 250μm in size was drilled by electro discharge machining from the center of the lower side of die plate, and then, micro die hole was accurately drilled by micro electro discharge machining process [14] from the center of upper side of die plate. Though we could not control the counter bore shape at its end, we believed that its round end, naturally formed by electro discharge drilling, would help in the structural safety of die hole. Structural analyses for die hole under maximum punch loads were also carried out, and their results showed that maximum von Mises stress was about 2.0GPa near the sharp edge of a die hole, and the deflections were found to be negligible compared with that of die hole dimensions. Fig.1-(b), (d), and (f) show the fabricated micro die holes. Tab.1 shows the measured diameter and roundness of fabricated punching tools.

2.2 Design and assembly of micro punching press

We made our efforts to meet two kinds of accuracy requirements of the press system. One was to ensure the highly accurate straight motion of a punch during hole piercing, and the other, the tool alignment accuracy. Since a 25μm hole punching under c/t=5% requires the punch-to-die clearance of only 1μm, both accuracies of the present press should be met within 1μm. We thought that the conventional die sets and press structure for hole piercing [11] could not meet both accuracies. Hence, a flexible system was designed in a way that a punch could have the vertical motion, and a die plate was to be mounted on movable x-y stepper so that horizontal position of die hole could be finely adjusted under a punch tip for tool alignment purpose, and it was verified with the help of a tool alignment teacher. Therefore, we mainly focused on ensuring highly straight motion of a punch. A high precision motion controller was used to control the punching press with submicron resolution.

Present press system was carefully designed with three basic design considerations. First, straight motion accuracy of a punch was to depend on only that of punch gripper mounted on highly accurate LM guide system. Second, Abbe error at punch tip was to be minimized. Third, we avoided any redundant constraints in the design of punch motion-driving part. The number of parts was also minimized considering assembly errors and process environment conditions. Fig.3 shows the present press assembly.

In the conventional piercing die set, the stripper works as a punch guide as well as a blank holder so that the lateral position accuracy of a punch motion can be guaranteed within the diametral tolerances of the punch shank and stripper hole. For this reason, even in the previous system [10], we had introduced the stripper as a punch guide as well as a blank holder in such a way that the second shank of punch was to be guided by a stripper hole. However, we thought that it was difficult to meet the horizontal position error of a punch tip within 1μm with such a guide system. In fact, in the previous press, the lateral position error of a punch tip randomly occurred within about ±2μm every punching process as schematically shown in Fig.2. It was inferred form the randomly formed eccentric burr of punched holes of 50μm in diameter. Hence, at the present design, we avoided the punch guide system by the stripper, but rather the lateral position error of a punch tip depended on only motion accuracy of punch gripper mounted on high precision LM guide system, and the stripper was to act as blank holder only. As the LM

guide, we used the off-the-shelf cross roller linear motion guide system with one axis and twin carriage structure, and its straightness and flatness accuracy was guaranteed within 1㎛/13mm. To accommodate the free motion of a punch tip, stripper hole of 500㎛ in diameter and 1.3mm in thickness was designed so that a stripper hole and punch did not interfere with each other. Increase of Abbe error at the punch tip was also minimized. (2) shows the maximum lateral position error of the punch tip in x- and y- directions by Abbe error when the punch is griped at the center of the punch gripper. After design optimization, we designed L_z and L_y in Fig.3 to be 2, and 3mm, respectively. Since the angular motion errors of the LM system used here were guaranteed to be less that about 20arcsec, $_x$, $_y$ could be reduced to submicron order.

$$\begin{aligned} \Delta_x &= L_z\Delta\theta_{y,yaw} + L_y\Delta\theta_{z,roll} \\ \Delta_y &= L_z\Delta\theta_{x,pitch} \end{aligned} \tag{2}$$

The punch motion-driving part was carefully designed based on a kinematic design principle [16] which means that redundant constraints could lead to lowering accuracy. Here, we introduced the push-pull mechanism similar to that of a manually driven linear positioning stage as shown in Fig.3. A log push rod is attached to an L-shaped plate mounted on vertical stepper. A push rod with round end rests against a punch griper. An extended spring is inserted between a punch gripper and a stripper. It pulls the punch gripper toward the push rod so that the punch gripper will always be held firmly against the push rod. When the vertical stepper moves downward, the push rod advances and pushes the punch gripper along the linear axis. When the vertical stepper moves up, a push rod retracts and a punch gripper follows because of the spring pressure holding the punch gripper against the end of push rod. Also, the relative vertical position of the stripper with respect to the punch tip is adjusted by a micrometer screw. To firmly grip the micro punch. V-groove was precisely machined and lapped on the punch gripper.

The lateral position error of a punch tip could be due to any slight lateral force during piercing. To visualize the phenomenon the structure of the designed press with a 25㎛ punch having the free length L_z of 2mm was analyzed. Here, the maximum lateral force applied at the tool tip was chosen under the assumption that this force would bring about maximum bending stress at the punch tip, 3.8GPa. Analysis results showed that the maximum lateral force was about 0.1N and corresponding defection at the punch tip was about 0.4㎛.

Present press was precisely assembled on the flat granite surface, minimizing the squareness error in both the punch motion axis and the vertical grip of a punch with respect to the die plate.

2.3 Two-way imaging system as a tool alignment teacher

The accurate alignment of 25㎛ tools with punch-to-die clearance of only 1㎛ was our challenging problem, which could only be done by finely adjusting the horizontal position of the die hole under a punch tip and observing the planar configuration of tool alignment with a vision system. We newly devised such a vision for our specific purpose, and named it at the two-way imaging system, because it can image the planer configuration of a tool alignment by optically combining images of both tool faces such as punch tip end and a die hole.

Fig.4-(a) shows the principle of the two-way image acquisition. The two-way imaging optic is composed of a polarizing cube beamsplitter (B_p), a mirror (M_2) coated $\lambda/4$ phase retarder (W), a tilting mirror (M_1), and a microscope. Coaxially illuminating lights from objective lens enter B_p via M_1 tilted by 30° with respect to the ground. Here, the tilting angle of M_1 was carefully determined considering the press geometry. B_p splits the incident beam into two highly polarized output separated by 90°. Reflected s-polarized lights leave the cube an illuminated the punch tip. The W and M_2 combination reversed the transmitted p-polarized beams and changes their

polarization angle into s-polarization, and they are reflected in a cube to illuminate a die plate. For imaging, reflected beams from both tool faces run back to an objective lens via inverse paths of illumination.

For a broadband purpose, a 50/50 polarizing cube beamsplitter made of SF1 having refractive index of 1.71 was used. As $\lambda/4$ phase retarder, a mica sheet was used because its birefringence varies slowly across the visible spectrum. To ensure the strength of the mica sheet, a glass-mica-glass combination having a total thickness if 2.2mm was used, and it was bonded to the rear face of a beamsplitter with the optical adhesive. The dielectric mirror was coated to ensure high reflectance of mirror M_2, and aluminum metal mirror was used as a tilting mirror (M_1) to minimize reflectance sensitivity to incidence angle of polarized light. For image magnification, we used a 10× plan apochromatic objective lens having a working distance and numerical aperture of 33.5mm, and 0.28, respectively, which gave diffraction-limited resolution of 1.2㎛ at 550nm wavelength. Pixel resolution was determined as 0.6㎛/pixel based on the principle that the minimum pixel size needed to resolve a structure is less than a half the radius of Airy disc [17]. Therefore, the primary magnification of 13× was chosen based on the relation between the pixel resolution and the primary magnification. A CCD camera with 1/3 in. format and 480 TV line resolution was used. Though we designed a two-way imaging optic for broadband purpose, we used the quasimonochromatic light source by the narrow band pass filter centered at 500nm to minimize chromatic aberration induced by a thick glass cube.

Cube size and its spatial position were carefully designed base on the geometrical optics theory. The basic design guide allowed a full light cone defined by the numerical aperture of objective lens within a cube. After design optimization, the cube size and the gap between cube bottom and die plate were designed to be 5, and 1.5mm, respectively, so that the distance between both tools at best focus was about 12.5mm. A tilting mirror was also designed to be 23.5×23.5×1mm in size with the same design guide for cube size determination.

A cube was to be precisely gripped and positioned on an optical mounting stage with five degrees of freedom in motions, xyz translation and two rotations in x- and y- directions. Fig.5 shows our vision system and micro punching press. Due to the refraction of light at the boundary of a cube and air, the tilting angle of a cube was to be adjusted. To adapt the two-way imaging optic to micro punching machine, the following procedures were done. We made a circular mark by punch indentation on brass foil and observed punch tip and its mark were to coincide exactly in combined image.

To ensure tool alignment accuracy of less that 1㎛, we introduced the image processing algorithm of the cross-correlation concept [17] which gives the similarity between two different images. A die hole was scanned around a punch tip, and at each sampling points, negated images of 25㎛ tools and artificially made white ring were cross correlated, and its peak value was stored. Scanning was done every 0.6㎛ interval, because pixel resolution in image was 0.6㎛. The total number of sampling points was 100. Here, the size of reference ring was determined with that of tools in an image. After scanning, we could find the best aligned tool configuration where the stored value would be maximal, that is, the tool clearance and artificially made ring would become most similar. Fig.4-(b) and (c) show planar configuration of 25㎛ tool alignment imaged by the developed vision system.

3. Fabrication results and discussion

After the tooling set was assembled and aligned on the micro punching press, the two-way imaging optic moved aside. Workpiece was inserted between stripper and die plate, and then

hole punching was performed. In this way, 100, 50, and 25㎛ holes were made under the same blanking condition, c/t=5%, respectively. Piercing was conducted at the punch speed of 10mm/sec, and no lubrication condition was used. As workpiece materials, commercially available brass CuZn37 and stainless steel 316 foils were used. The thickness of the workpiece foil was to be 100, 50, 25㎛, respectively, to accommodate the hole fabrication with a depth-to-diameter ratio of one.

To investigate the hole quality, dimensional and shape accuracies of fabricated holes such as the hole size, roundness, straightness, and hole tapering were defined as seen in Fig.6, and they were measured and analyzed, considering the general shape of the mechanically pierced holes [9] such as rollover, burnish, fracture, and burr. For this, the upper side and lower one of the pierced holes, and their sections were observed and measured with the microscope and commercial measuring software. Measurements were done with five specimens for each fabricated holes and they were averaged. Fig.7 and Tab. 2 show their fabrication results.

Fabrication results showed that the mechanical punching process could reproducibly make accurate holes even in micro scale application. Very clean and round holes were observed on the upper side of the work metals, and roundness accuracy and hold size (DU) were found to be almost the same with those of the punch tips, regardless of workpiece materials. Also, for all cases, hole straightness was measured to be less than 1㎛, and the rollover depth (DR) was within 5~6% of workpice thickness. Hole tapering and burr formation were found to be related with the fracture behavior of the pierced holes. As schematically shown in Fig.6, the standard blanking process generally leads to a hole with the ductile fracture areas produced by the crack initiation and propagation [13] at the end of punching process so that breakout diameter (DL) becomes larger than the burnish diameter (DU) and hole tapering increases. In this case, burr formation was dominated by tensile fracture. In fact, such fracture zones were observed in brass holes of 100, and 50㎛ in diameter and stainless steel hole of 100㎛ in diameter. For those holes, the tapering angle was measured to be 1~2°, and burr height per workpiece thickness was around 1.5~2%. However the brass hole of 25㎛ in diameter, and stainless hole of 25 and 50㎛ in diameter do not have such a fracture area, rather almost full shearing seems to occur as seen the inner surface of fabricated holes of Fig.7-(c) and (f).

We estimated such phenomenon was due to relatively large size of grains compared with the thickness of workpiece metals. That is, the average grain size of both work metals were about 10㎛, and there were 2~3 grains in workpiece foils of 25㎛ in thickness along punching direction. In this case, the typical mechanisms of ductile fracture by piercing, crack initiation and propagation, do not seem to work. But rather shear deformation is dominated along the hole wall and the scrap is separated from work metal by the tearing at the end of hole piercing. Therefore, in the hole fabrication of less than a certain critical size on a given work metal, the hole shape mainly depends on the punch tip geometry so that burnish diameter (DU) and breakout one (DL) become almost same, and hole tapering is enhanced. However, the percent of burr size to workpiece thickness was found to be relatively large, 3~4%, which is about same with the ratio of the die clearance to workpiece thickness, 5%. Stainless steel holes of 50㎛ in diameter evidently show such tendency. The burnish diameter and breakout one are almost same, and hole tapering was enhanced to be 0.2°, and burr height to workpiece thickness was about 4%. Also, 25㎛ holes on both work metals also show the consistent feature about hole tapering and burr formation. Hole tapering was measure to be -1° and burr height to workpiece thickness was about 3~4%. Here, hole tapering of -1° was seemed to result from the tapered geometry of a 25㎛ punch tip. Edge profiles of 25㎛ holes show that the material flows aside at the upper side of pierced holes due to the penetration of 25㎛ punch tip with a tapered geometry.

4. Conclusions

In this study, micro hole fabrication by mechanical punching process was studied. Basically, we tried to control both the feature size and process condition, and scaled it down to 25㎛ hole punching process. For this, micro punching system was developed considering the accuracy requirements for 25㎛ hole fabrication, and 100, 50, 25㎛ holes were successfully made on brass, and stainless steel foils, respectively, under the standard blanking condition, c/t=5%.
Fabrication results showed that mechanical punching process could reproducibly make accurate holes even in micro scale application. Up to around 100㎛ hole punching, hole qualities such as hole tapering and burr formation were affected by the conventional fracture behavior. However, in the hole fabrication of less than a certain critical size on a given work metal, hole features were different from those of conventional punched holes, and hole qualities mainly depended on tool geometry rather than workpiece material. Possibly, micro hole fabrications below 25㎛ can be made with our punching machine under more careful process design. Of course, the accurate fabrication of micro tools should be preceded.
Future works in this area could include the following: First, productivity enhancement of micro punching process should be studied. Second, the effect of grain by grain deformation on punched hole quality should be exploited, because it would be help in better understanding the micro punching mechanism.

5. Acknowledgement

This work was supported by Korea Institute of Industrial Technology. Micro die holes were fabricated by the micro EDM system in Prof. C.N. Chu's laboratory. Their helps are gratefully acknowledged.

6. References

[1] Y. Saotome, S. Miwa, T. Zhang, and A. Inoue, The micro-formability of Zr-based amorphous alloys in the supercooled liquid state and their application to micro-dies, JMPT, Vol. 113, 2001, pp. 64-99
[2] Y. Saotome, and H. Iwazhki, Superplastic backward microextrusion of microparts for micro-electro-mechanical systems, JMPT, Vol. 119, 2001, pp. 307-311
[3] Ike, M. Plancak, Coining process as a means of controlling surface micro geometry, JMPT, Vol. 80-81, 1998, pp. 101-107
[4] J. Boehm, A. Schubert. T. Otto, and T. Burkhardt, Micro-metalforming with silicon dies, Microsystem Technologies, Vol 7, 2001, pp. 191-195
[5] Y. Saotome, T. Okamoto, An in-situ incremental microforming system for three-dimensional shell structures of foil materials, JMPT, Vol. 113, 2001, pp. 636-640
[6] U. Engel, R. Eckstein, Microforming-from basic research to its realization, JMPT, Vol. 125-126, 2002, pp. 35-34
[7] Masuzawa, T., Fujino, M., A process for manufacturing very fine pin tools, SME Techincal paper, MS90-307, 1990
[8] T. Mori, K. Hirota, D. Tokumoto, Improvement of ultra-fine piercing by vacuum system", Int. symposium on IEEE MHS, 2000, pp. 77-82
[9] Metals Handbook, Vol 14, Forming and Forging, ASM, 1988
[10] B. Y. Joo, S. I. Oh, and B. H. Jeon, Development of Micro Punching System, Annals of the

CIRP, Vol. 50/1, 2001, pp191~194
[11] Ivana Suchy, Hand book of die design, McGraw-Hill, 1997
[12] M. Geiger, F. Vollertsen, R. Kals, Fundamentals on the manufacturing of sheet metal microparts, Annals of the CIRP, Vol. 34/1, 1996, pp. 277-282
[13] S. Y. Luo, Effect of the geometry and the surface treatment of punching tools on the tool life and wear conditions in the piercing of thick steel plate, JMPT, Vol. 88, 1999, pp. 122-133
[14] G. M. Kim, B. H. Kim, C. N. Chu, 1999, Machining Rate and Electro Wear Characteristics in Micro-EDM of Micro-Holes, J. of the Korea Society of Precision Engineering, Vol. 16/10, pp. 94-100.
[15] Eric H. K Fung, and S.M. Yang, An approach to on-machine motion error measurement of a linear slide, Measurement, Vol. 29, 2001, pp. 51-62
[16] P. Schmiechen, and A. Slocum, Analysis of kinematic systems: a generalized approach, Precision Engineering, Vol. 19, 1996, pp. 11-18
[17] E. Hecht, Optics, Addison-Wesley, 1998

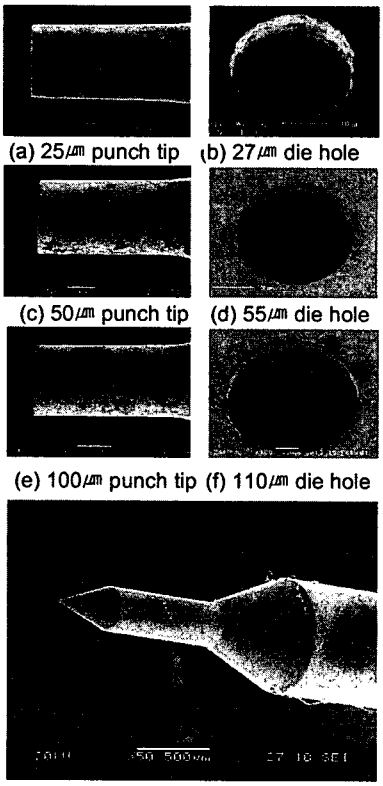

Figure 1 : Tungsten carbide micro punching tools

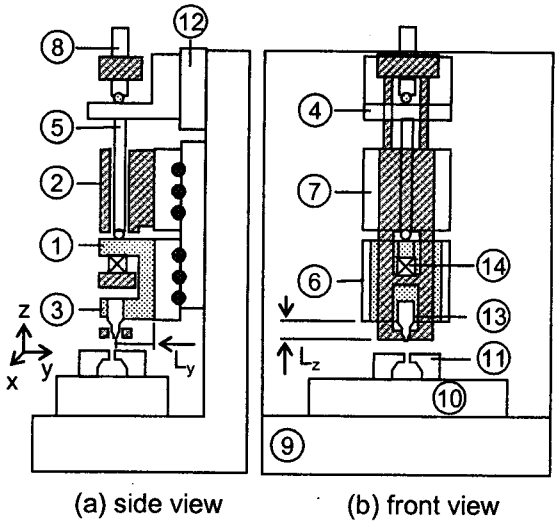

	hole size (㎛)	tool diameter (㎛)	roundness (㎛)
punch tip	25	24~25	< 0.3
die hole		26.5~27.5	< 0.6
punch tip	50	49.5~50.5	<0.4
die hole		55~56	< 0.9
punch tip	100	99~100	< 0.8
die hole		110~111.5	< 1.1

Table 1 : Size and roundness of micro punching tool

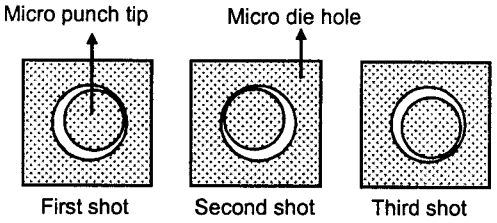

Figure 2: Lateral position error of punch tip

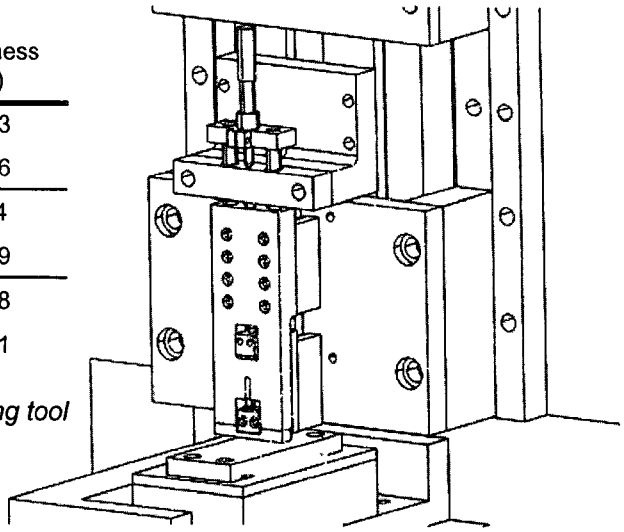

Figure 3: Micro punching press assembly

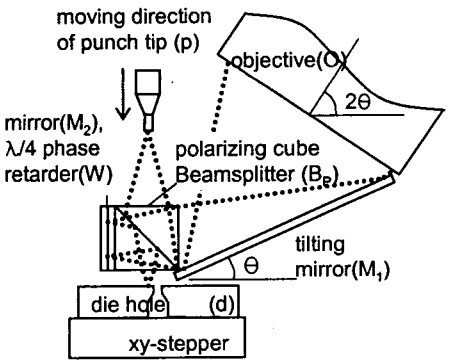

(a) Two-way imaging optic as a tool alignment teacher

(b) Misaligned tools (c) Well aligned tools

Figure 4 : Alignment of 25㎛ punching tools

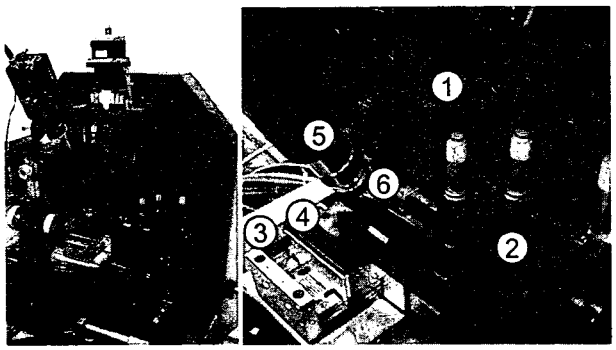

1. Punch motion-driving part
2. Optical stage
3. xy- stepper

Figure 5: Micro press and tool alignment helper

	Brass	Brass	Brass	AISI 316	AISI 316	AISI 316
tool size(㎛)	100	50	25	100	50	25
round. (㎛)	0.7	0.4	0.3	0.7	0.4	0.3
straight.(㎛)	<1	<1	<1	<1	<1	<1
tapering (°)	1.7	1.1	-1.1	2.2	0.2	-0.9
DU(㎛)	101.4	50.8	26.8	100.9	50.9	26.8
DL(㎛)	107	52.5	25.8	109	51.3	26
DR(㎛)	4.7	1.3	-	1.1	3.3	-
DB(㎛)	91.4	42.9	25	77.7	46.6	25
DF(㎛)	8.6	5.7	-	22.2	-	-
HB/thick.(%)	<1.4	<2	<3.4	<1.5	<4	<3

Table 2 : Measurement results for micro hole quality

25㎛ hole 50㎛ hole 100㎛ hole
(a) Upper side of brass CuZn37

25㎛ hole 50㎛ hole 100㎛ hole
(b) Lower side of brass CuZn37

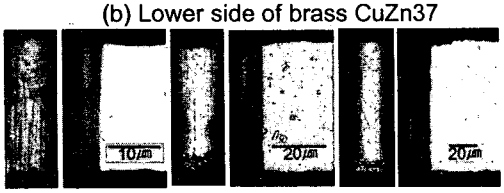

25㎛ hole 50㎛ hole 100㎛ hole
(c) Inner surface and hole edge (brass CuZn37)

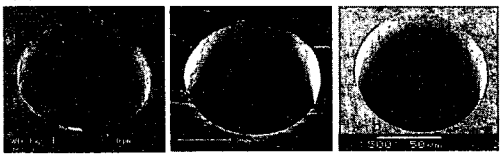

25㎛ hole 50㎛ hole 100㎛ hole
(d) Upper side of AISI 316

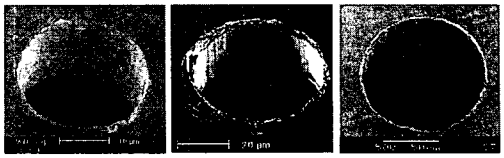

25㎛ hole 50㎛ hole 100㎛ hole
(e) Lower side of AISI 316

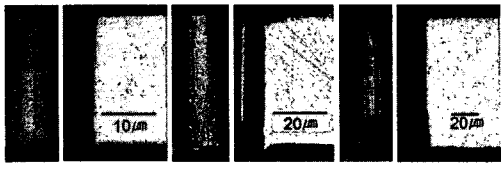

25㎛ hole 50㎛ hole 100㎛ hole
(f) Inner surface and hole edge (AISI 316)

Figure 7 : Mechanically pierced micro holes

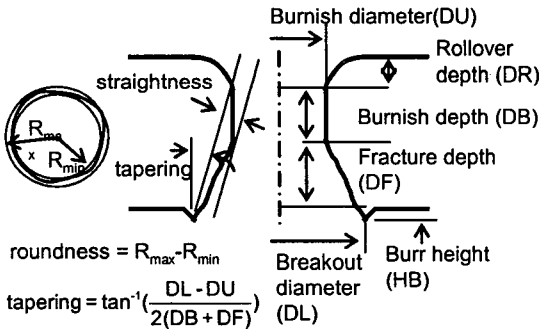

Figure 6 : Measuring parameters for punched hole